Morphological processing of univariate Gaussian distribution-valued images based on Poincaré upper-half plane representation

Jesus Angulo, Santiago Velasco-Forero

▶ **To cite this version:**

Jesus Angulo, Santiago Velasco-Forero. Morphological processing of univariate Gaussian distribution-valued images based on Poincaré upper-half plane representation. 2013. hal-00795012v1

HAL Id: hal-00795012

https://minesparis-psl.hal.science/hal-00795012v1

Preprint submitted on 27 Feb 2013 (v1), last revised 22 Jan 2015 (v3)

HAL is a multi-disciplinary open access archive for the deposit and dissemination of scientific research documents, whether they are published or not. The documents may come from teaching and research institutions in France or abroad, or from public or private research centers.

L'archive ouverte pluridisciplinaire **HAL**, est destinée au dépôt et à la diffusion de documents scientifiques de niveau recherche, publiés ou non, émanant des établissements d'enseignement et de recherche français ou étrangers, des laboratoires publics ou privés.

Morphological processing of univariate Gaussian distribution-valued images based on Poincaré upper-half plane representation

Jesús Angulo[a] , Santiago Velasco-Forero[b]

[a] CMM-Centre de Morphologie Mathématique, Mathématiques et Systèmes, MINES ParisTech; France

[b] ITWM - Fraunhofer Institute, Kaiserlautern, Germany

jesus.angulo@mines-paristech.fr,velascoforero@itwm.fraunhofer.de

February 2013

Abstract

Mathematical morphology is a nonlinear image processing methodology based on the application of complete lattice theory to spatial structures. Let us consider an image model where at each pixel is given a univariate Gaussian distribution. This model is interesting to represent for each pixel the measured mean intensity as well as the variance (or uncertainty) for such measurement. The aim of this paper is to formulate morphological operators for these images by embedding Gaussian distribution pixel values on the Poincaré upper-half plane. More precisely, it is explored how to endow this classical hyperbolic space with various families of partial orderings which lead to a complete lattice structure. Properties of order invariance are explored and application to morphological processing of univariate Gaussian distribution-valued images is illustrated.

Keywords: Ordered Poincaré half plane, hyperbolic partial ordering, hyperbolic complete lattice, mathematical morphology, Gaussian-distribution valued image, information geometry image filtering

1 Introduction

This work is motivated by the exploration of a mathematical image model f where instead of having a scalar intensity $t \in \mathbb{R}$ at each pixel p, i.e., $f(p) = t$, we have a univariate Gaussian probability distribution of intensities $N(\mu, \sigma^2) \in \mathcal{N}$, i.e., image f is defined as the function

$$f : \left\{ \begin{array}{ccc} \Omega & \rightarrow & \mathcal{N} \\ p & \mapsto & N(\mu, \sigma^2) \end{array} \right.$$

where Ω is the support space of pixels p (e.g., for 2D images $\Omega \subset \mathbb{Z}^2$) and $\mathcal{N}$ denotes the family of univariate Gaussian probability distribution functions (pdf). Nowadays most of imaging sensors only produces single scalar values since the CCD (charge-coupled device) cameras typically integrates the light (arriving photons) during a given exposure time τ. To increase the signal-to-noise ratio (SNR), exposure time is increased to $\tau' = \alpha\tau$, $\alpha > 1$. Let suppose that α is a positive integer number, this is equivalent to a multiple acquisition of α frames during τ for each frame (i.e., a kind of temporal oversampling). The standard approach only considers the sum (or average) of the multiple intensities [19], without taking into account the variance which is a basic estimator of the noise useful for probabilistic image processing. Another example of such a representation from a gray scale image consists in considering that each pixel is described by the mean and the variance of the intensity distribution from its centered patch.

Henceforth, the corresponding image processing operators should be able to deal with Gaussian distributions-valued pixels. In particular, morphological operators for images $f \in \mathcal{F}(\Omega, \mathcal{N})$ involves that the space of Gaussian distributions $\mathcal{N}$ must be endowed of a partial ordering leading to a complete lattice structure. In practice, it means that given a set of Gaussian pdfs, as the example given in Fig. 1, we need to be able to define a Gaussian pdf which corresponds to the infimum (inf) of the set and another one to the supremum (sup). Mathematical morphology is a nonlinear image processing methodology based on the computation of sup/inf-convolution filters (i.e., dilation/erosion operators) in local neighborhoods [22]. Mathematical morphology is theoretically formulated in the framework of complete lattices and operators defined on them [20, 13]. When only the supremum or the infimum are well defined, other morphological operators can be formulated in the framework of complete semilattices [15, 14]. Both cases are considered here for images $f \in \mathcal{F}(\Omega, \mathcal{N})$.

A possible way to deal with the partial ordering problem of $\mathcal{N}$ can be founded on stochastic ordering (or stochastic dominance) [21] which is basically defined in terms of majorization of cumulative distribution functions.

However, we prefer to adopt here an information geometry approach [2], which is based on considering that the univariate Gaussian pdfs are points in a hyperbolic space. More generally, Fisher geometry amounts to hyperbolic geometry of constant curvature for other location-scale families of probability distributions (Cauchy, Laplace, elliptical) $p(x; \mu, \sigma) = \frac{1}{\sigma} f(\frac{x-\mu}{\sigma})$, where curvature depends on the dimension and the density profile [7, 8]. For a deep flavor on hyperbolic geometry see [5]. There are several models representing the hyperbolic space in $\mathbb{R}^d$, $d > 1$, such as the three following ones: the (Poincaré) upper half-space model $\mathcal{H}^d$, the Poincaré disk model $\mathcal{P}^d$ and the Klein disk model $\mathcal{K}^d$.

1. The (Poincaré) upper half-space model is the domain $\mathcal{H}^d = \{(x_1, \cdots, x_d) \in \mathbb{R}^d \mid x_d > 0\}$ with the Riemannian metric $ds^2 = \frac{dx_1^2 + \cdots + dx_d^2}{x_d^2}$;

2. The Poincaré disk model is the domain $\mathcal{P}^d = \{(x_1, \cdots, x_d) \in \mathbb{R}^d \mid \ x_1^2 + \cdots + x_d^2 < 1\}$

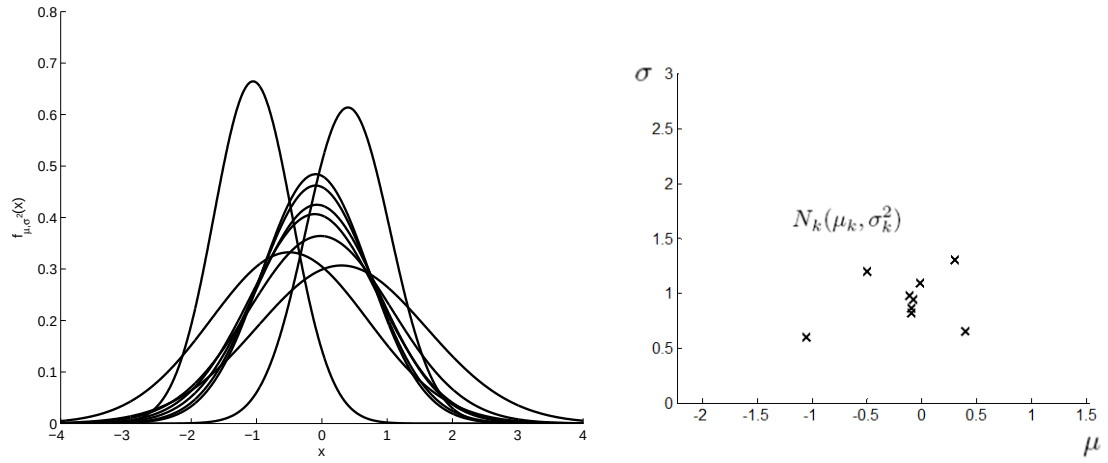

Figure 1: (a) Example of a set of nine univariate Gaussian pdfs, $N_k(\mu_k, \sigma_k^2)$, $1 \leq k \leq 9$. (b) Same set of Gaussian pdfs represented as points of coordinates (μ_k, σ_k) in the upper-half plane.

with the Riemannian metric $ds^2 = 4\frac{dx_1^2+\cdots+dx_d^2}{(1-x_1^2-\cdots-x_d^2)^2}$;

3. The Klein disk model is the space $\mathcal{K}^d = \{(x_1, \cdots, x_d) \in \mathbb{R}^d \mid x_1^2 + \cdots + x_d^2 < 1\}$ with the Riemannian metric $ds^2 = \frac{dx_1^2+\cdots+dx_d^2}{1-x_1^2-\cdots-x_d^2} + \frac{(x_1dx_1+\cdots+x_ddx_d)^2}{(1-x_1^2-\cdots-x_d^2)^2}$.

These models are isomorphic between them in the sense that one-to-one correspondences can be set up between the points and lines in one model to the points and lines in the other so as to preserver the relations of incidence, betweenness and congruence. In particular, there exists an isometric mapping between any pair among these models and analytical transformations to convert from one to other are well known [5, 18]. In this paper, we focus on the simplest Poincaré half-plane model, $\mathcal{H}^2$, which is sufficient for our practical purposes of manipulating Gaussian pdfs. Fig. 1(b) illustrates the example of a set of nine Gaussian pdfs $N_k(\mu_k, \sigma_k^2)$ represented as points of coordinates (μ_k, σ_k) in the upper-half plane.

In summary, from a theoretical viewpoint, the aim of this paper is to endow $\mathcal{H}^2$ with partial orderings which lead to useful invariance properties in order to formulate appropriate morphological operators for images $f : \Omega \to \mathcal{H}^2$. The rest of the paper is organized as follows. Section 2 reminds the basics on the geometry of Poincaré half-plane model. Then, various partial orderings on $\mathcal{H}^2$ are studied in Section 3. Based on the corresponding complete lattice structure of $\mathcal{H}^2$, Section 4 presents definition of morphological operators for images on $\mathcal{F}(\Omega, \mathcal{H}^2)$ and its application to morphological processing univariate Gaussian distribution-valued images. Section 5 concludes the paper with the perspectives of the present work.

2 Geometry of Poincaré upper-half plane $\mathcal{H}^2$

In complex analysis, the upper-half plane is the set of complex numbers with positive imaginary part:

$$\mathcal{H}^2 = \{z = x + iy \in \mathbb{C} \mid \ y > 0\}\,. \tag{1}$$

We use also the notation $x = \Re(z)$ and $y = \Im(z)$. The boundary of upper-half plane (called sometimes circle at infinity) is the real axis together with the infinity, i.e., $\partial\mathcal{H}^2 = \mathbb{R} \cup \infty = \{z = x + iy \mid \ y = 0, x = \pm\infty, y = \infty\}$.

2.1 Riemannian metric, angle and distance

In hyperbolic geometry, the Poincaré upper-half plane model (originated with Beltrami and also known as Lobachevskii space in Soviet scientific literature) is the space $\mathcal{H}^2$ together with the Poincaré metric $(g_{kl}) = \text{diag}\left(\frac{1}{y^2} \quad \frac{1}{y^2}\right)$ such that the hyperbolic arc length is given by

$$ds^2 = \sum_{k,l=1,2} g_{kl}\, dx\, dy = \frac{dx^2 + dy^2}{y^2}. \tag{2}$$

With this metric, the Poincaré upper-half plane is a complet Riemannian manifold of sectional curvature equal to -1. The tangent space to $\mathcal{H}^2$ at a point z is defined as the space of tangent vectors at z. It has the structure of a 2-dimensional real vector space, $T_z\mathcal{H}^2 \simeq \mathbb{R}^2$. The Riemannian metric (2) is induced by the following inner product on $T_z\mathcal{H}^2$: for $\zeta_1, \zeta_2 \in T_z\mathcal{H}^2$, with $\zeta_k = (\xi_k, \eta_k)$, we put

$$\langle \zeta_1, \zeta_2 \rangle_z = \frac{(\zeta_1, \zeta_2)}{\Im(z)^2} \tag{3}$$

which is a scalar multiple of the Euclidean inner product $(\zeta_1, \zeta_2) = \xi_1\xi_2 + \eta_1\eta_2$.

The angle θ between two geodesics in $\mathcal{H}^2$ at their intersection point z as the angle between their tangent vectors in $T_z\mathcal{H}^2$, i.e.,

$$cos\theta = \frac{\langle \zeta_1, \zeta_2 \rangle_z}{\|\zeta_1\|_z \|\zeta_2\|_z} = \frac{(\zeta_1, \zeta_2)}{\sqrt{(\zeta_1, \zeta_1)}\sqrt{(\zeta_2, \zeta_2)}}. \tag{4}$$

We see that this notion of angle measure coincides with the Euclidean angle measure. Consequently, the Poincaré upper-half plane is a conformal model.

The distance between two points $z_1 = x_1 + iy_1$ and $z_2 = x_2 + iy_2$ in $\left(\mathcal{H}^2, ds^2\right)$ is the function

$$\text{dist}_{\mathcal{H}^2}(z_1, z_2) = \cosh^{-1}\left(1 + \frac{(x_1 - x_2)^2 + (y_1 - y_2)^2}{2y_1y_2}\right) \tag{5}$$

Distance (5) is derived from the logarithm of the cross-ratio between these two points and the points at the infinity, i.e., $\text{dist}_{\mathcal{H}^2}(z_1, z_2) = \log D(z_1^\infty, z_1, z_2, z_2^\infty)$ where $D(z_1^\infty, z_1, z_2, z_2^\infty) = \frac{z_1 - z_2^\infty}{z_1 - z_1^\infty}\frac{z_2 - z_1^\infty}{z_2 - z_2^\infty}$. To obtain their equivalence, we remind that $\cosh^{-1}(x) = \log(x + \sqrt{x^2 - 1})$.

From this formulation is easy to check that for two points with $x_1 = x_2$ the distance is $\text{dist}_{\mathcal{H}^2}(z_1, z_2) = \left|\log\left(\frac{y_1}{y_2}\right)\right|$.

To see that $\text{dist}_{\mathcal{H}^2}(z_1, z_2)$ is a metric distance in $\mathcal{H}^2$, we first notice the argument of $\cosh^{-1}$ always lies in $[1, \infty)$ and $\cosh(x) = \frac{e^x + e^{-x}}{2}$, so cosh is increasing and concave on $[0, \infty)$. Thus $\cosh^{-1}(1) = 0$ and $\cosh^{-1}$ is increasing and concave down on $[1, \infty)$, growing logarithmically. The properties required to be a metric (non-negativity, symmetry and triangle inequality) are proven using the cross-ratio formulation of the distance.

We note that the distance from any point $z \in \mathcal{H}^2$ to $\partial\mathcal{H}^2$ is infinity.

Remark. *Distance between two univariate Gaussian pdfs.* Given two univariate Gaussian pdfs $N(\mu_1, \sigma_1^2)$ and $N(\mu_2, \sigma_2^2)$, the Fisher distance between them, $\text{dist}_{Fisher} : \mathcal{N} \times \mathcal{N} \to \mathbb{R}_+$, defined from the Fisher information metric [2], is given by [7]:

$$\text{dist}_{Fisher}\left((\mu_1, \sigma_1^2), (\mu_2, \sigma_2^2)\right) = \sqrt{2}\text{dist}_{\mathcal{H}^2}\left(\frac{\mu_1}{\sqrt{2}} + i\sigma_1, \frac{\mu_2}{\sqrt{2}} + i\sigma_2\right), \tag{6}$$

which shows how hyperbolic geometry arises naturally from the Fisher information metric.

2.2 Geodesics

The geodesics of $\mathcal{H}^2$ are the vertical lines, $VL(a) = \{z \in \mathcal{H}^2 \mid \Re(z) = a\}$, and the semi-circles in $\mathcal{H}^2$ which meet the horizontal axis $\Re(z) = 0$ orthogonally, $SC_r(a) = \{z \in \mathcal{H}^2 \mid |z - z'| = r;\ \Re(z') = a \text{ and } \Im(z') = 0\}$; see Fig 2(a). In particular, given any pair $z_1, z_2 \in \mathcal{H}^2$, there is a unique geodesic connecting them, or in other terms, given these two points with $x_1 \neq x_2$ there exist a unique semi-circle of center $c = (a, 0)$, radius r, and being orthogonal to x-axis, i.e., $(z_1, z_2) \mapsto SC_{r_{1\frown 2}}(a_{1\frown 2})$ where

$$a_{1\frown 2} = \frac{x_2^2 - x_1^2 + y_2^2 - y_1^2}{2(x_2 - x_1)}; \quad r_{1\frown 2} = \sqrt{(x_1 - a_{1\frown 2})^2 + y_1^2} = \sqrt{(x_2 - a_{1\frown 2})^2 + y_2^2}. \tag{7}$$

More precisely, the unique geodesic parameterized by the length, $t \mapsto \gamma(z_1, z_2; t)$, $\gamma : [0, 1] \to \mathcal{H}^2$ joining two points $z_1 = x_1 + iy_1$ and $z_2 = x_2 + iy_2$ such as $\gamma(z_1, z_2; 0) = z_1$ and $\gamma(z_1, z_2; 1) = z_2$ is given by

$$\gamma(z_1, z_2; 0) = \begin{cases} x_1 + ie^{\xi t + t_0} & \text{if} \quad x_1 = x_2 \\ [r\tanh(\xi t + t_0) + a] + i\left[\frac{r}{\cosh(\xi t + t_0)}\right] & \text{if} \quad x_1 \neq x_2 \end{cases} \tag{8}$$

with a and r given in (7) and where for $x_1 = x_2$, $t_0 = \log(y_1)$, $\xi = \log\frac{y_2}{y_1}$ and for $x_1 \neq x_2$

$$t_0 = \cosh^{-1}\left(\frac{r}{y_1}\right) = \sinh^{-1}\left(\frac{x_1 - a}{y_1}\right), \ \xi = \log\left(\frac{y_1}{y_2}\frac{r + \sqrt{r^2 - y_2^2}}{r + \sqrt{r^2 - y_1^2}}\right).$$

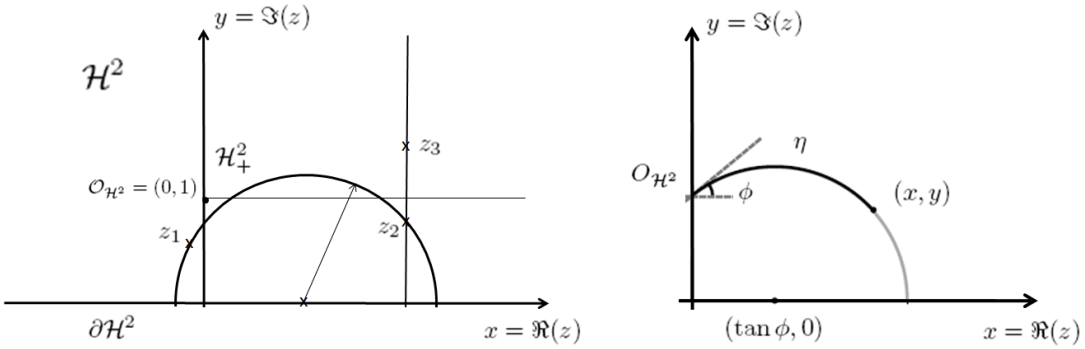

Figure 2: (a) Geodesics of $\mathcal{H}^2$: z_1 and z_2 are connected by a unique semi-circle; the geodesic between z_2 and z_3 is a segment of vertical line. (b) Hyperbolic polar coordinates.

Remark. *Interpolation between two univariate normal distributions.* Using the closed-form expression of geodesics $t \mapsto \gamma(z_1, z_2; t)$, given in (8), it is possible to compute the average univariate Gaussian pdf between $N(\mu_1, \sigma_1^2)$ and $N(\mu_2, \sigma_2^2)$, with $(\mu_k = x_k, \sigma_k = y_k)$, by taking $t = 0.5$. More generally, we can interpolate a series of distributions between them by discretizing t between 0 and 1. An example of such method is given in Fig. 3. We note in particular that the average Gaussian pdf can have a variance bigger than σ_1^2 and σ_2^2. We note also that, due to the "logarithmic scale" of imaginary axis, equally spaces points in t do not have equal Euclidean arc-length in the semi-circle.

2.3 Hyperbolic polar coordinates

The position of point $z = x + iy$ in $\mathcal{H}^2$ can be given either in terms of Cartesian coordinates (x, y) or by means of polar hyperbolic coordinates (η, ϕ), where η represents the distance of the point from the origin $\mathcal{O}_{\mathcal{H}^2} = (0, 1)$ and ϕ represents the slope of the tangent in $\mathcal{O}_{\mathcal{H}^2}$ to the geodesic (i.e., semi-circle) joining the point (x, y) with the origin. The formulas which relate the hyperbolic coordinates (η, ϕ) to the Cartesian ones (x, y) are [4]

$$\begin{cases} x = \frac{\sinh\eta\cos\phi}{\cosh\eta - \sinh\eta\sin\phi}, & \eta > 0 \\ y = \frac{1}{\cosh\eta - \sinh\eta\sin\phi}, & -\frac{\pi}{2} < \phi < \frac{\pi}{2} \end{cases} \qquad \begin{cases} \eta = \mathrm{dist}_{\mathcal{H}^2}(\mathcal{O}_{\mathcal{H}^2}, z) \\ \phi = \arctan\frac{x^2+y^2-1}{2x} \end{cases} \tag{9}$$

We notice that the center of the geodesic passing trough (x, y) from $\mathcal{O}_{\mathcal{H}^2}$ has Cartesian coordinates given by $(\tan\phi, 0)$; see Fig 2(b).

2.4 Isometric symmetry

Let the projective special linear group defined by $\mathrm{PSL}(2, \mathbb{R}) = \mathrm{SL}(2, \mathbb{R})/\{\pm \mathrm{I}\}$ where the special linear group $\mathrm{SL}(2, \mathbb{R})$ consists of 2×2 matrices with real entries whose determinant

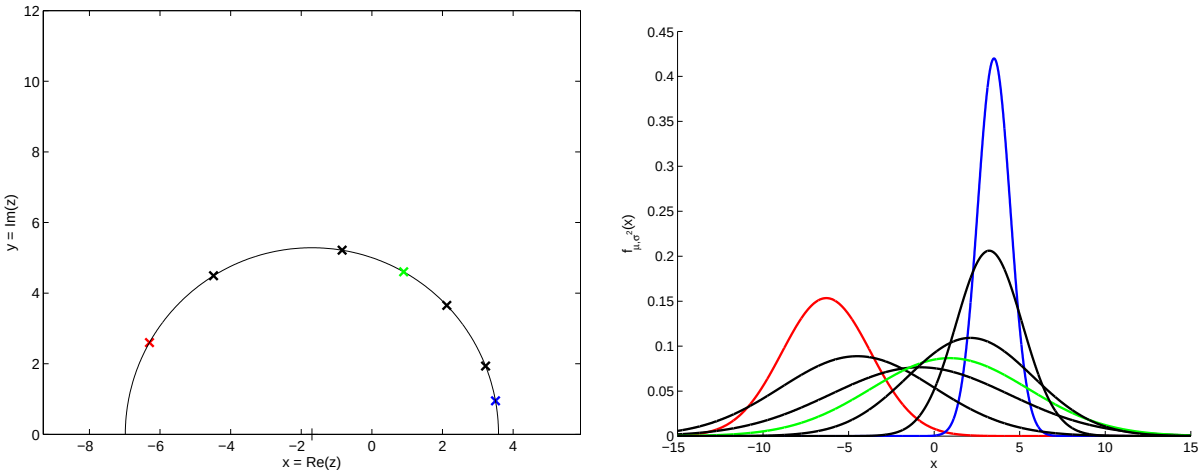

(a) (b)

Figure 3: (a) Example of interpolation of 5 points in $\mathcal{H}^2$ between points $z_1 = -6.3 + i2.6$ (in red) and $z_2 = 3.5 + i0.95$ (in blue) using their geodesic $t \mapsto \gamma(z_1, z_2; t)$, with $t = 0.2$, 0.4, 0.5, 0.6, 0.8. The average point (in green) corresponds just to $\gamma(z_1, z_2; 0.5) = 0.89 + i4.6$. (b) Original (in red and blue) univariate Gaussian pdfs and corresponding interpolated ones.

equals $+1$, i.e.,

$$g \in \mathrm{SL}(2, \mathbb{R}) : \quad g = \begin{pmatrix} a & b \\ c & d \end{pmatrix}, \; ad - bc = 1;$$

and I denotes the identity matrix. This defines the group of Möbius transformations $M_g : \mathcal{H}^2 \to \mathcal{H}^2$ by setting for each $g \in \mathrm{SL}(2, \mathbb{R})$,

$$z \mapsto M_g(z) = \begin{pmatrix} a & b \\ c & d \end{pmatrix} \cdot z = \frac{az + b}{cz + d} = \frac{ac|z|^2 + bd + (ad + bc)\Re(z) + i\Im(z)}{|cz + d|^2}$$

The Lie group $\mathrm{PSL}(2, \mathbb{R})$ acts on the upper half-plane by preserving the hyperbolic distance, i.e.,

$$\mathrm{dist}_{\mathcal{H}^2}(M_g(z_1), M_g(z_2)) = \mathrm{dist}_{\mathcal{H}^2}(z_1, z_2), \; \forall g \in \mathrm{SL}(2, \mathbb{R}), \; \forall z_1, z_2 \in \mathcal{H}^2.$$

This includes both orientation preserving isometries. The orientation-reversing (mirror map, i.e., $z = x + iy \mapsto -\bar{z} = -x + iy$) isometries involves a determinant equals -1.

Note the action of group $\mathrm{PSL}(2, \mathbb{R})$ is transitive, in the sense that $z_1, z_2 \in \mathcal{H}^2$, there exists a $g \in \mathrm{PSL}(2, \mathbb{R})$ (in general not unique) such that $gz_1 = z_2$. The stabilizer or isotropy subgroup of an element in $\mathcal{H}^2$ is the set of $g \in \mathrm{PSL}(2, \mathbb{R})$ which leave z unchanged $gz = z$. The stabilizer of $z = i$ is the rotation group $\mathrm{SO}(2)$.

Let $H \in \mathcal{H}^2$ be a geodesic of the upper half-plane, which is described uniquely by its endpoints in $\partial\mathcal{H}^2$, there exists a Möbius transformation M_g such that M_g maps H bijectively

to the imaginary axis, i.e., $VL(0)$. If H is the vertical line $VL(a)$, the transformation is the translation $z \mapsto M_g(z) = z - a$. If H is the semi-circle $SC_r(a)$ with endpoints in real axis are $\zeta_-, \zeta_+ \in \mathbb{R}$, where $\zeta_- = a - r$ and $\zeta_+ = a + r$, the map is given by $M_g(z) = \frac{z-\zeta_-}{z-\zeta_+}$, such that $M_g(\zeta_-) = 0$, $M_g(\zeta_+) = \infty$ and $M_g(a + ir) = i$.

The unit-speed geodesic going up vertically, through the point $z = i$ is given by

$$\gamma(t) = \begin{pmatrix} e^{t/2} & 0 \\ 0 & e^{-t/2} \end{pmatrix} \cdot i = ie^t.$$

Because $\mathrm{PSL}(2, \mathbb{R})$ acts transitively by isometries of the upper half-plane, this geodesic is mapped into other geodesics through the action of $\mathrm{PSL}(2, \mathbb{R})$. Thus, the general unit-speed geodesic is given by

$$\gamma(t) = \begin{pmatrix} a & b \\ c & d \end{pmatrix} \begin{pmatrix} e^{t/2} & 0 \\ 0 & e^{-t/2} \end{pmatrix} \cdot i = \frac{aie^t + b}{cie^t + d}.$$

2.5 Hyperbolic circles

Let consider an Euclidean circle of center $c = (x_c, y_c) \in \mathcal{H}^2$ and radius r in the upper-half plane, defined as $C_r(c) = \{z \in \mathcal{H}^2 | \sqrt{(x_c - a)^2 + (y_c - b)^2} = r\}$, such that it is contained in the upper-half plane, i.e., $C_r(c) \subset \mathcal{H}^2$. The corresponding hyperbolic circle $C_{\mathcal{H}^2, r_h}(c_h)$ $\{z \in \mathcal{H}^2 | \mathrm{dist}_{\mathcal{H}^2}(c_h, z) = r_h\}$ is geometrically equal to $C_r(c)$ but its hyperbolic center and radius are given by

$$c_h = (x_c,\ \sqrt{y_c^2 - r^2}); \quad r_h = \tanh^{-1}\left(\frac{r}{y_c}\right).$$

We note that the hyperbolic center is always below the Euclidean center. The inverse equations are

$$c = (x_c = x_h,\ y_c = y_h \cosh r_h); \quad r = y_h \sinh r_h.$$

Remark. *Minimax center in $\mathcal{H}^2$.* Finding the smallest circle that contains all of a set of points $x_1, x_2 \cdots, x_N$ in the Euclidean plane is a classical problem in computational geometry, called the minimum enclosing circle MEC. It is also relevant is statistical estimation since the unique center of the circle c^∞ (called 1-center or minimax center) is defined as the L^∞ center of mass, i.e., for $\mathbb{R}^2$, $c^\infty = \arg\min_{x \in \mathbb{R}^2} \max_{1 \leq i \leq N} \|x_i - x\|_2$. Computing the smallest enclosing sphere in Euclidean spaces is intractable in high dimensions, but efficient approximation algorithms have been proposed. The Bădoiu and Clarkson algorithm [3] leads to a fast and simple approximation (of known precision ϵ after a given number of iterations $\lceil \frac{1}{\epsilon^2} \rceil$ using the notion of core-set, but independent of dimensionality n). The computation of the minimax center is particularly relevant in information geometry (smallest enclosing information disk [17]) and has been considered for hyperbolic models such as the Klein disk, using a Riemannian extension of Bădoiu and Clarkson algorithm [1], which only requires

a closed-form of the geodesics. Fig. 4 depicts an example of minimax center computation using Bădoiu and Clarkson algorithm for a set of univariate Gaussian pdfs represented in $\mathcal{H}^2$. We note that, using this property of circle preservation, computation the minimal enclosing hyperbolic circle of a given set of points $Z = \{z_k\}_{1 \leq k \leq K}$, $z_k \in \mathcal{H}^2$, denoted $MEC_{\mathcal{H}^2}(Z)$ is equivalent to computing the corresponding minimal enclosing circle $MEC(Z)$ if and only if we have $MEC(Z) \subset \mathcal{H}^2$. This is the case for the example given in Fig. 4.

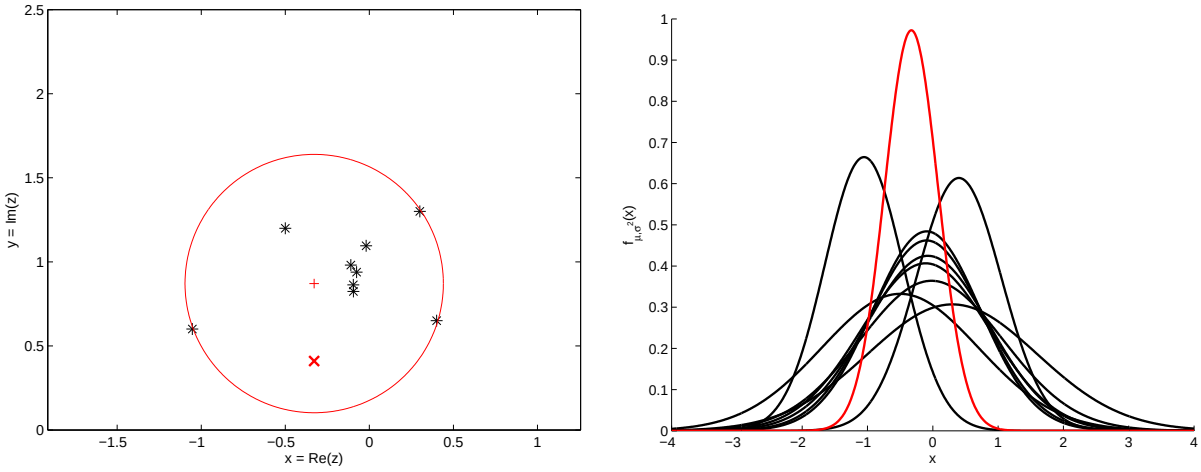

(a) (b)

Figure 4: (a) Example of minimax center (x_h, y_h) (red $\times$) of a set of nine points $Z = \{z_k\}_{1 \leq k \leq 9}$ in H^2 (original points $*$ in black), the minimal enclosing circle $MEC_{\mathcal{H}^2}(Z)$ of is also depicted (in red). (b) Corresponding minimax center Gaussian set $N(\mu = x_h, \sigma^2 = y_h^2)$ of nine univariate Gaussian pdfs, $N_k(\mu_k, \sigma_k^2)$, $1 \leq k \leq 9$.

3 Endowing $\mathcal{H}^2$ with partial ordering and its complete (inf-semi)lattice structures

The notion of ordering invariance in the Poincaré upper-half plane was considered in the Soviet literature [11, 12]. Ordering invariance with respect to simple transitive subgroup T of the group of motions was studied, i.e., group T consists of transformations t of the form: $z = x + iy \mapsto z' = (\lambda x + \alpha) + i\lambda y$, where $\lambda > 0$ and α are real numbers. We named T the Guts group. However, up to the best of our knowledge, the formulation of partial orders on Poincaré upper-half plane has not been widely study. We introduce here partial orders in $\mathcal{H}^2$ and study invariance properties to transformations of Guts group or to subgroups of $\mathrm{SL}(2, \mathbb{R})$ (Möbius transformations).

3.1 Upper half-plane product ordering

A real vector space E on which a partial order $\leq$ is given (reflexive, transitive, antisymmetric) is called an ordered vector space if (i) $x, y, z \in E$ and $x \leq y$ implies $x+z \leq y+z$; (ii) $x, y \in E$, $0 \leq \lambda \in \mathbb{R}$, and $x \leq y$ implies $\lambda x \leq \lambda y$. An element $x \in E$ with $x \geq 0$ (that means that all the vector components are positive) is said to be positive. The set $E_+ = \{x \in E \mid x \geq 0\}$ for all positive elements is called the cone of positive elements. It turns out that the order of an ordered vector space is determined by the set of positive elements. Let E be a vector space and $C \subset E$ a cone. Then, $x \leq y$ if $x - y \in C$ defines an order on E such that E is an ordered vector space with $E_+ = C$. The notion of partially ordered vector space is naturally extended to partially ordered groups [10]. An ordered vector space E is called a vector lattice $(E, \leq)$ if $\forall x, y \in E$ there exist the joint (supremum or least upper bound) $x \vee y = \sup(x, y) \in E$ and the meet (infimum or greatest lower bound) $x \wedge y = \inf(x, y) \in E$. A vector lattice is also called a Riesz space.

Thus, we can introduce a similar order structure in $\mathcal{H}^2$ as a product order of $\mathbb{R} \times \mathbb{R}_+$. To achieve this goal, we need to define, on the one hand, the equivalent of ordering preserving linear combination. More precisely, given tree points $z_1, z_2, z_3 \in \mathcal{H}^2$ and a scalar positive number $0 \leq \lambda \in \mathbb{R}$ we say that

$$z_1 \leq_{\mathcal{H}^2} z_2 \text{ implies } \lambda \boxdot z_1 \boxplus z_3 \leq_{\mathcal{H}^2} \lambda \boxdot z_2 \boxplus z_3,$$

where we have introduced the following pair of operations in $\mathcal{H}^2$:

$$\lambda \boxdot z = \lambda x + i y^{\lambda} \text{ and } z_1 \boxplus z_2 = (x_1 + x_2) + i(y_1 y_2).$$

On the other hand, the corresponding partial ordering $\leq_{\mathcal{H}^2}$ will be determined by the positive cone in $\mathcal{H}^2$ defined by $\mathcal{H}^2_+ = \{z \in \mathcal{H}^2 \mid x \geq 0 \text{ and } y \geq 1\}$, i.e.,

$$z_1 \leq_{\mathcal{H}^2} z_2 \Leftrightarrow z_2 \boxminus z_1 \in \mathcal{H}^2_+, \tag{10}$$

with $z_2 \boxminus z_1 = (x_2 - x_1) + i(y_2^{-1} y_1)$. According to this partial ordering the corresponding supremum and infimum for any pair of points z_1 and z_2 in $\mathcal{H}^2$ are naturally defined as follows

$$z_1 \vee_{\mathcal{H}^2} z_2 = (x_1 \vee x_2) + i \exp\left(\log(y_1) \vee \log(y_2)\right), \tag{11}$$

$$z_1 \wedge_{\mathcal{H}^2} z_2 = (x_1 \wedge x_2) + i \exp\left(\log(y_1) \wedge \log(y_2)\right). \tag{12}$$

Therefore $\mathcal{H}^2$ endowed with partial ordering (10) is a complete lattice, but it is not bounded since the the greatest (or top) and least (or bottom) elements are in the boundary $\partial\mathcal{H}^2$. We also have a duality between supremum and infimum, i.e.,

$$z_1 \vee_{\mathcal{H}^2} z_2 = \complement\left(\complement z_1 \wedge_{\mathcal{H}^2} \complement z_2\right); \quad z_1 \wedge_{\mathcal{H}^2} z_2 = \complement\left(\complement z_1 \vee_{\mathcal{H}^2} \complement z_2\right),$$

with respect to the following involution

$$z \mapsto \complement z = (-1) \boxdot z = -x + i y^{-1}. \tag{13}$$

We easily note that, in fact, $\exp(\log(y_1) \vee \log(y_2)) = y_1 \vee y_2$ and similarly for the infimum, since the logarithm is an isotone mapping (i.e., monotone increasing) and therefore order-preserving. Therefore, the partial ordering $\leq_{\mathcal{H}^2}$ does not involve any particular structure for $\mathcal{H}^2$ and does not take into account the Riemannian nature of the upper half plane. According to that, we note also that the partial ordering $\vee_{\mathcal{H}^2}$ is invariant to the Guts group of transforms.

3.2 Upper half-plane symmetric ordering

Let us consider a symmetrization of the product ordering with respect to the origin in the upper half-plane. Given any pair points $z_1, z_2 \in \mathcal{H}^2$, we define the upper half-plane symmetric ordering as

$$z_1 \preceq_{\mathcal{H}^2} z_2 \Leftrightarrow \begin{cases} 0 \leq x_1 \leq x_2 & \text{and} \quad 0 \leq \log(y_1) \leq \log(y_2) & \text{or} \\ x_2 \leq x_1 \leq 0 & \text{and} \quad 0 \leq \log(y_1) \leq \log(y_2) & \text{or} \\ x_2 \leq x_1 \leq 0 & \text{and} \quad \log(y_2) \leq \log(y_1) \leq 0 & \text{or} \\ 0 \leq x_1 \leq x_2 & \text{and} \quad \log(y_2) \leq \log(y_1) \leq 0 & \end{cases} \tag{14}$$

The four conditions of this partial ordering entails that only points belonging the same quadrant of $\mathcal{H}^2$ can be ordered, where the four quadrants $\{\mathcal{H}^2_{++}, \mathcal{H}^2_{-+}, \mathcal{H}^2_{--}, \mathcal{H}^2_{+-}\}$ are defined with respect to the origin $\mathcal{O}_{\mathcal{H}^2} = (0, 1)$ which corresponds to the pure imaginary complex $z_0 = i$. In other words, we can summarize the partial ordering (14) by saying that if z_1 and z_2 belongs to the same $\mathcal{O}$-quadrant of $\mathcal{H}^2$ we have $z_1 \preceq_{\mathcal{H}^2} z_2 \Leftrightarrow |x_1| \leq |x_2|$ and $|\log(x_1)| \leq |\log(x_2)|$. Endowed with the partial ordering (14), $\mathcal{H}^2$ becomes a partially ordered set (poset) where the bottom element is z_0, but we notice that there is not top element. In addition, for any pair of point z_1 and z_2 the infimum $\curlywedge_{\mathcal{H}^2}$ is given by

$$z_1 \curlywedge_{\mathcal{H}^2} z_2 \Leftrightarrow \begin{cases} (x_1 \wedge x_2) + i(y_1 \wedge y_2) & \text{if } z_1, z_2 \in \mathcal{H}^2_{++} \\ (x_1 \vee x_2) + i(y_1 \wedge y_2) & \text{if } z_1, z_2 \in \mathcal{H}^2_{-+} \\ (x_1 \vee x_2) + i(y_1 \vee y_2) & \text{if } z_1, z_2 \in \mathcal{H}^2_{--} \\ (x_1 \wedge x_2) + i(y_1 \vee y_2) & \text{if } z_1, z_2 \in \mathcal{H}^2_{+-} \\ z_0 & \text{otherwise} \end{cases} \tag{15}$$

The infimum (15) extends naturally to any finite set of points in $\mathcal{H}^2$, $Z = \{z_k\}_{1 \leq k \leq K}$, and will be denoted by $\bigwedge_{\mathcal{H}^2} Z$. However, the supremum $z_1 \curlyvee_{\mathcal{H}^2} z_2$ is not defined; or more precisely, it is defined if and only if z_1 and z_2 belongs to the same quadrant, i.e., similarly to (15) mutatis mutandis $\wedge$ by $\vee$ with the "otherwise" case as "non existent". Consequently, the poset $(\mathcal{H}^2, \preceq_{\mathcal{H}^2})$ is only a complete inf-semilattice. The fundamental property of such infimum (15) if its self-duality with respect to involution (13), i.e.,

$$z_1 \curlywedge_{\mathcal{H}^2} z_2 = \complement\left(\complement z_1 \curlywedge_{\mathcal{H}^2} \complement z_2\right). \tag{16}$$

Due to the strong dependency of partial ordering $\preceq_{\mathcal{H}^2}$ with respect to $\mathcal{O}_{\mathcal{H}^2}$, it is easy to see that such ordering is only invariant to transformations that does not move points from one quadrant to another one. This is the case typically for mappings as $z \mapsto \lambda \boxdot z$, $\lambda > 0$.

3.3 Upper half-plane polar ordering

Previous order $\preceq_{\mathcal{H}^2}$ is only a partial ordering, and consequently given any pair of points z_1 and z_2, the infimum can be not defined or, even if defined, can be different from z_1 and z_2. Let us introduce a total ordering in $\mathcal{H}$ based on hyperbolic polar coordinates, which takes into account also an ordering relationship with respect to $\mathcal{O}_{\mathcal{H}^2}$. Thus, given two points $\forall z_1, z_2 \in \mathcal{H}$ the upper half-plane polar ordering states

$$z_1 \leq^{pol}_{\mathcal{H}^2} z_2 \Leftrightarrow \begin{cases} \eta_1 < \eta_2 & \text{or} \\ \eta_1 = \eta_2 & \text{and} \quad \tan\phi_1 \leq \tan\phi_2 \end{cases} \tag{17}$$

The polar supremum $z_1 \vee^{pol}_{\mathcal{H}^2} z_2$ and infimum $z_1 \wedge^{pol}_{\mathcal{H}^2} z_2$ are naturally defined from the order (17) for any subset of points Z, denoted by $\bigvee^{pol}_{\mathcal{H}^2} Z$ and $\bigwedge^{pol}_{\mathcal{H}^2} Z$. Total order $\leq^{pol}_{\mathcal{H}^2}$ leads to a complete lattice, bounded from the bottom (i.e., the origin $\mathcal{O}_{\mathcal{H}^2}$) but not from the top. Furthermore, as $\leq^{pol}_{\mathcal{H}^2}$ is a total ordering, the supremum and the infimum will be either z_1 or z_2.

Polar total order is invariant to any Möbius transformation M_g which preserves the distance to the origin (isometry group) and more generally to isotone maps in distance, i.e., $\eta(z_1) \leq \eta(z_2) \Leftrightarrow \eta(M_g(z_1)) \leq \eta(M_g(z_2))$ but which also preserves the orientation order, i.e., order on the polar angle. This is for instance the case of orientation group SO(2) and the scaling maps $z \mapsto M_g(z) = \lambda z$, $0 < \lambda \in \mathbb{R}$.

We note also that instead of considering as origin $\mathcal{O}_{\mathcal{H}^2}$, the polar hyperbolic coordinates can be defined with respect to a different origin $z_0^{'}$ and consequently, the total order is adapted to the new origin (i.e., bottom element is just $z_0^{'}$).

3.4 Upper half-plane geodesic ordering

As discussed above, there is a unique hyperbolic geodesic joining any pair of points. Given two points $z_1, z_2 \in \mathcal{H}^2$ such that $x_1 \neq x_2$, let $SC_{r_{1\frown 2}}(a_{1\frown 2})$ be the semi-circle defining their geodesic, where the center $a_{1\frown 2}$ and the radius $r_{1\frown 2}$ are given by Eqs. (9). Let denote by $z_{1\frown 2}$ the point of $SC_{r_{1\frown 2}}(a_{1\frown 2})$ having maximal imaginary part, i.e., its imaginary part is equal to the radius: $z_{1\frown 2} = a_{1\frown 2} + ir_{1\frown 2}$.

The upper half-plane geodesic ordering $\preceq^{geo}_{\mathcal{H}^2}$ defines an order for points being in the same half of their geodesic semi-circle as follows,

$$z_1 \preceq^{geo}_{\mathcal{H}^2} z_2 \Leftrightarrow \begin{cases} a_{1\frown 2} \leq x_1 < x_2 & \text{or} \\ x_2 < x_1 \leq a_{1\frown 2} \end{cases} \tag{18}$$

Property of transitivity of this partial ordering, i.e., $z_1 \preceq^{geo}_{\mathcal{H}^2} z_2$, $z_2 \preceq^{geo}_{\mathcal{H}^2} z_3 \rightarrow z_1 \preceq^{geo}_{\mathcal{H}^2} z_3$, holds for points belonging to the same geodesic. For two points in a geodesic vertical line, $x_1 = x_2$, we have $z_1 \preceq^{geo}_{\mathcal{H}^2} z_2 \Leftrightarrow y_2 \leq y_1$. According to this partial ordering, we define the geodesic infimum, denoted by $\curlywedge^{geo}_{\mathcal{H}^2}$, as the point on the geodesic joining z_1 and z_2 with

maximal imaginary part, i.e., for any $z_1, z_2 \in \mathcal{H}^2$, with $x_1 \neq x_2$, we have

$$z_1 \curlywedge_{\mathcal{H}^2}^{geo} z_2 \Leftrightarrow \begin{cases} (x_1 \vee x_2) + i(y_1 \vee y_2) & \text{if} \quad x_1, x_2 \leq a_{1\frown 2} \\ (x_1 \wedge x_2) + i(y_1 \vee y_2) & \text{if} \quad x_1, x_2 \geq a_{1\frown 2} \\ z_{1\frown 2} & \text{otherwise} \end{cases} \tag{19}$$

If $x_1 = x_2$, we have that $z_1 \curlywedge_{\mathcal{H}^2}^{geo} z_2 = x_1 + i(y_1 \vee y_2)$. In any case, we have that $\text{dist}_{\mathcal{H}^2}(z_1, z_2) = \text{dist}_{\mathcal{H}^2}(z_1, z_1 \curlywedge_{\mathcal{H}^2}^{geo} z_2) + \text{dist}_{\mathcal{H}^2}(z_1 \curlywedge_{\mathcal{H}^2}^{geo} z_2, z_2)$. Intuitively, we notice that the geodesic infimum is the point of the geodesic farthest from the real line.

We observe that if one attempts to define the geodesic supremum from the partial ordering $\preceq_{\mathcal{H}^2}^{geo}$, it results that the supremum is not defined for any pair of points, i.e., supremum between z_1 and z_2 is defined only if and only if both points are in the same half of its semi-circle. To tackle this limitation, we propose to define the geodesic supremum $z_1 \curlyvee_{\mathcal{H}^2}^{geo} z_2$ by duality with respect to the involution $\complement z$ introduced in (13), i.e.,

$$z_1 \curlyvee_{\mathcal{H}^2}^{geo} z_2 = \complement \left(\complement z_1 \curlywedge_{\mathcal{H}^2}^{geo} \complement z_2 \right) \Leftrightarrow \begin{cases} (x_1 \wedge x_2) + i(y_1 \wedge y_2) & \text{if} \quad x_1, x_2 \leq a_{1\frown 2} \\ (x_1 \vee x_2) + i(y_1 \wedge y_2) & \text{if} \quad x_1, x_2 \geq a_{1\frown 2} \\ \complement z_{\complement 1 \frown \complement 2} & \text{otherwise} \end{cases} \tag{20}$$

where $\complement z_{\complement 1 \frown \complement 2}$ is the dual point associated to the semi-circle defined by dual points $\complement z_1$ and $\complement z_2$.

Nevertheless, in order to have a structure of complete lattice for $(\mathcal{H}^2, \preceq_{\mathcal{H}^2}^{geo})$, it is required that the infimum and the supremum of any set of points $Z = \{z_k\}_{1 \leq k \leq K}$ with $K > 2$, are well defined. Namely, according to (19), the geodesic infimum of Z, denoted $\bigwedge_{\mathcal{H}^2}^{geo} Z$, corresponds to the point z_{inf} with maximal imaginary part on all possible geodesics joining any pair of points $z_n, z_m \in Z$. In geometric terms, that means that between all these geodesics, there exists one which gives z_{inf}. Instead of computing all the geodesics, we propose to define the infimum $\bigwedge_{\mathcal{H}^2}^{geo} Z$ as the point $z_{\text{inf}} = a_{\text{inf}} + ir_{\text{inf}}$, where a_{inf} is the center of the smallest semi-circle in $\mathcal{H}^2$ of radius r_{inf} which encloses all the points in the set Z. We have the following property

$$\bigwedge_{\mathcal{H}^2}^{geo} Z = z_{\text{inf}} \preceq_{\mathcal{H}^2}^{geo} z_k, \;\; 1 \leq k \leq K,$$

which geometrically means that the geodesic connecting z_{inf} to any point z_k of Z lies always in one of the half part of the semi-circle defined by z_{inf} and z_k.

In practice, the minimal enclosing semi-circle defining z_{inf} can be easily computed by means of the following algorithm based on the minimum enclosing Euclidean circle MEC of a set of points: (1) Working on $\mathbb{R}^2$, define a set of points given, on the one hand, by Z and, on the other hand, by Z^* which corresponds to the reflected points with respect to x-axis (complex conjugate), i.e., points $Z = (x_k, y_k)$ and points $Z^* = (x_k, -y_k)$, $1 \leq k \leq K$; (2) Compute the $MEC(Z \cup Z^*) \mapsto C_r(c)$, in such a way that, by symmetric point configuration, we necessarily have the center on the x-axis, i.e., $c = (x_c, 0)$; (3) The infimum $\bigwedge_{\mathcal{H}^2}^{geo} Z = z_{\text{inf}}$

is given by $z_{\text{inf}} = x_c + ir$. Fig. 5(a)-(b) gives an example of computation of the geodesic infimum from a set of points in $\mathcal{H}^2$.

As for the case of two points, the geodesic supremum of Z is defined by duality with respect to involution (13), i.e.,

$$z_{\text{sup}} = \bigvee_{\mathcal{H}^2}^{geo} Z = \complement \left(\bigwedge_{\mathcal{H}^2}^{geo} \complement Z \right) = a_{\text{sup}} + i r_{\text{sup}}, \tag{21}$$

with $a_{\text{sup}} = -x_c^{dual}$ and $r_{\text{sup}} = 1/r^{dual}$, where $SC_{r^{dual}}(x_c^{dual})$ is the minimal enclosing semi-circle from dual set of points $\complement Z$. According to this formulation by duality we have that, for any $Z \subset \mathcal{H}^2$,

$$z_{\text{inf}} \preceq_{\mathcal{H}^2}^{geo} z_{\text{sup}},$$

which is a consequence of the fact z_{sup} lies inside the semi-circle defined by z_{inf}. An example of computing the geodesic supremum z_{sup} is also given in Fig. 5(a)-(b).

It is easy to see that geodesic infimum and supremum have the following properties: (i) $\Im(z_{\text{inf}}) \geq \Im(z_k)$ and $\Im(z_{\text{sup}}) \leq \Im(z_k)$, $\forall z_k \in Z$; (ii) $\bigvee_{1 \leq k \leq K} \Re(z_k) < \Re(z_{\text{inf}}), \Re(z_{\text{sup}}) < \bigwedge_{1 \leq k \leq K} \Re(z_k)$. The proofs are straightforward from the notion of minimal enclosing semi-circle.

Geodesic infimum and supremum being defined by minimal enclosing semi-circles, their invariance properties are related to homothetic transformations as well as translation on x-axis. That corresponds just to the Guts group of transformations.

3.5 Upper half-plane asymmetric geodesic infimum/supremum

According to the properties of geodesic infimum z_{inf} and supremum z_{sup} discussed above, we note that their real parts $\Re(z_{\text{inf}})$ and $\Re(z_{\text{sup}})$ belong to the interval bounded by the real parts of points of set Z. Moreover, $\Re(z_{\text{inf}})$ and $\Re(z_{\text{sup}})$ are not ordered between them. Therefore, the real part of supremum can be smaller than that of the infimum. For instance, in the extreme case of a set Z where all the imaginary parts are equal, the real part of its geodesic infimum and supremum are both equal to the average of the real parts of points, i.e., given $Z = \{z_k\}_{1 \leq k \leq K}$, if $y_k = y$, $1 \leq k \leq K$, then $\Re(z_{\text{inf}}) = \Re(z_{\text{sup}}) = 1/K \sum_{k=1}^{K} x_k$. From the viewpoint of morphological image filtering, it can be potentially interesting to impose an asymmetric behavior for the infimum and supremum such that $\Re(z_{\text{inf}}^{-\rightarrow+}) \leq z_k \leq \Re(z_{\text{sup}}^{-\rightarrow+})$, $1 \leq k \leq K$. Note that the proposed notation $- \rightarrow +$ indicates a partially ordered set on x-axis. In order to fulfil these requirements, we can geometrically consider the rectangle bounding the minimal enclosing semi-circle, which is just of dimensions $2r_{\text{inf}} \times r_{\text{inf}}$, and use it to define the asymmetric infimum $z_{\text{inf}}^{-\rightarrow+}$ as the upper-left corner of the rectangle. The asymmetric supremum $z_{\text{sup}}^{-\rightarrow+}$ is similarly defined from the bounding rectangle of the dual minimal enclosing semi-circle. Mathematically, given the geodesic infimum z_{inf} and supremum z_{sup}, we have the following definitions for the asymmetric geodesic infimum and

supremum:

$$\begin{cases} z_{\text{inf}}^{-\rightarrow+} = \bigvee_{\mathcal{H}^2}^{-\rightarrow+} Z = (a_{\text{inf}} - r_{\text{inf}}) + i r_{\text{inf}}; \\ z_{\text{sup}}^{-\rightarrow+} = \bigwedge_{\mathcal{H}^2}^{-\rightarrow+} Z = -(x_c^{dual} - r^{dual}) + i \frac{1}{r^{dual}}. \end{cases} \tag{22}$$

Remark. *Geodesic infimum and supremum of Gaussian distributions.* Let us consider their interpretation as infimum and supremum of a set of univariate Gaussian pdfs, see example depicted in Fig. 5. Given a set of K Gaussian pdfs $N_k(\mu = x_k, \sigma^2 = y_k^2)$, $1 \leq k \leq K$, we observe that the Gaussian pdf associated to the geodesic infimum $N_{\text{inf}}(\mu = x_{\text{inf}}, \sigma^2 = y_{\text{inf}}^2)$ has a variance larger than any Gaussian of the set and its mean is a kind of barycenter between the Gaussian pdfs having larger variance. The supremum Gaussian pdf $N_{\text{sup}}(\mu = x_{\text{sup}}, \sigma^2 = y_{\text{sup}}^2)$ has smaller variance than the K Gaussian pdfs and its mean is between the ones of small variance. In terms of the corresponding cumulative distribution functions, we observe that geodesic supremum/infimum do not have a natural interpretation. In the case of the asymmetric Gaussian geodesic infimum $N_{\text{inf}}^{-\rightarrow+}(\mu = x_{\text{inf}}^{-\rightarrow+}, \sigma^2 = (y_{\text{inf}}^{-\rightarrow+})^2)$ and Gaussian supremum $N_{\text{sup}}^{-\rightarrow+}(\mu = x_{\text{sup}}^{-\rightarrow+}, \sigma^2 = (y_{\text{sup}}^{-\rightarrow+})^2)$, we observe how the means are ordered with respect to the K others, which involves also that the corresponding cdfs are ordered. The latter is related to the notion of stochastic dominance [21] and will be explored in detail in ongoing research.

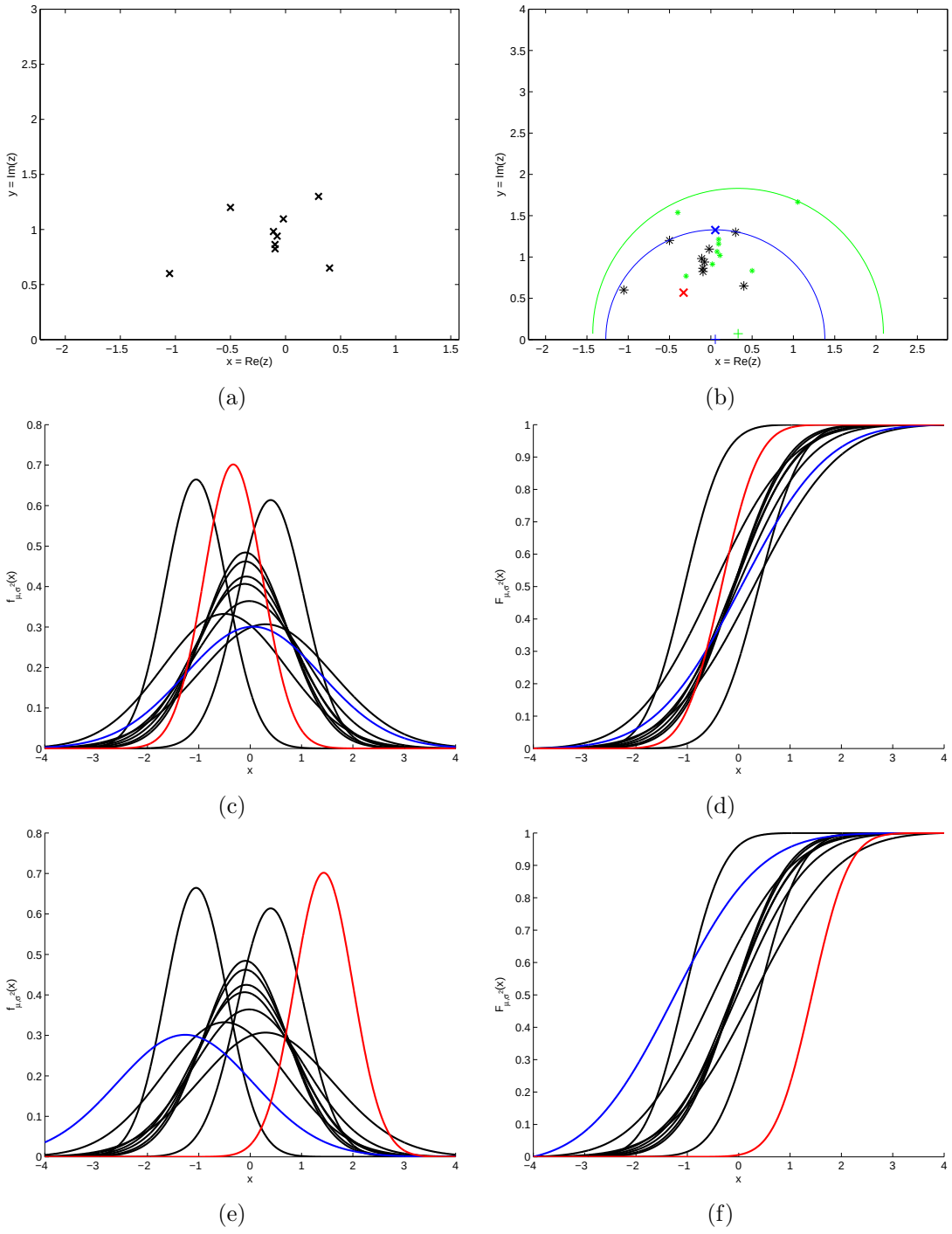

Figure 5: (a) Set of nine points in $\mathcal{H}^2$, $Z = \{z_k\}_{1 \leq k \leq 9}$. (b) Computation of infimum $\bigwedge_{\mathcal{H}^2}^{geo} Z = z_{\text{inf}}$ (blue "$\times$") and supremum $\bigvee_{\mathcal{H}^2}^{geo} Z = z_{\text{sup}}$ (red "$\times$"). Black "$*$" are the original points and green "$*$" the corresponding dual ones. (c) In black, set of Gaussian pdfs associated to Z, i.e., $N_k(\mu = x_k, \sigma^2 = y_k^2)$; in green, infimum Gaussian pdf $N_{\text{inf}}(\mu = x_{\text{inf}}, \sigma^2 = y_{\text{inf}}^2)$; in red, supremum Gaussian pdf $N_{\text{inf}}(\mu = x_{\text{inf}}, \sigma^2 = y_{\text{inf}}^2)$. (d) Cumulative distribution functions of Gaussian pdfs from (c). (e) Infimum and supremum Gaussian pdfs (in green and red respectively) from asymmetric geodesic infimum $z_{\text{inf}}^{-\rightarrow+}$ and $z_{\text{sup}}^{-\rightarrow+}$.

4 Morphological operators on $\mathcal{F}(\Omega, \mathcal{H}^2)$ for processing univariate Gaussian distribution-valued images

Let consider that $\mathcal{H}^2$ has been endowed with one of the partial orderings discussed above, denoted generally by $\leq$. Hence $(\mathcal{H}^2, \leq)$ is a poset, which has also a structure of complete lattice since we consider that the infimum $\bigwedge$ and supremum $\bigvee$ are defined for any set of points in $\mathcal{H}^2$. We note that for the symmetric ordering $\preceq_{\mathcal{H}^2}$ one has only an inf-semilattice structure.

4.1 Adjunction on complete lattice $(\mathcal{H}^2, \leq)$

The operators $\varepsilon : \mathcal{H}^2 \to \mathcal{H}^2$ and $\delta : \mathcal{H}^2 \to \mathcal{H}^2$ are an erosion and a dilation if they commute respectively with the infimum and the supremum: $\varepsilon\left(\bigwedge_k z_k\right) = \bigwedge_k \varepsilon(z_k)$ and $\delta\left(\bigvee_k z_k\right) = \bigvee_k \delta(z_k)$, for every set $\{z_k\}_{1 \leq k \leq K}$. Erosion and dilation are increasing operators, i.e., $\forall z, z' \in \mathcal{H}^2$, if $z \leq z'$ then $\varepsilon(z) \leq \varepsilon(z')$ and $\delta(z) \leq \delta(z')$. Erosion and dilation are related by the notion of adjunction [20, 13], i.e., $\forall z, z' \in \mathcal{H}^2$, $\delta(z) \leq z' \Leftrightarrow z \leq \varepsilon(z')$. Adjunction law is of fundamental importance in mathematical morphology since it allows to define a unique dilation δ associated to a given erosion ε, i.e., $\delta(z') = \bigwedge\{z \in \mathcal{H}^2 \ : \ z' \leq \varepsilon(z)\}$, $z' \in \mathcal{H}^2$. Similarly one can define a unique erosion from a given dilation: $\varepsilon(z) = \bigvee\{z' \in \mathcal{H}^2 \ : \ \delta(z') \leq z\}$, $z \in \mathcal{H}^2$. Given an adjunction (ε, δ), we also have the guarantee that their product operators, $\gamma(z) = \delta\left(\varepsilon(z)\right)$ and $\varphi(z) = \varepsilon\left(\delta(z)\right)$ are respectively an opening and a closing, which are the basic morphological filters having very useful properties [20, 13]: idempotency $\gamma\gamma(z) = \gamma(z)$, anti-extensivity $\gamma(z) \leq z$ and extensivity $z \leq \varphi(z)$, and increaseness. Another relevant result is the fact, given an erosion ε, the opening and closing by adjunction are exclusively defined in terms of the erosion [13] as $\gamma(z) = \bigwedge\left\{z' \in \mathcal{H}^2 \ : \ \varepsilon(z) \leq \varepsilon(z')\right\}$, $\varphi(z) = \bigwedge\left\{\varepsilon(z') \ : \ z' \in \mathcal{H}^2 \, , \ z \leq \varepsilon(z')\right\}$, $\forall z \in \mathcal{H}^2$.

In the case of complete inf-semilattice $(\mathcal{H}^2, \leq)$, where the infimum $\bigvee$ is defined but the supremum $\bigvee$ is not necessarily so, have the following particular results [15, 14]: (a) it is always possible to associate an opening γ to a given erosion ε by means of $\gamma(z) = \bigwedge\left\{z' \in \mathcal{H}^2 \ : \ \varepsilon(z) \leq \varepsilon(z')\right\}$, (b) even though the adjoint dilation δ is not well-defined in $\mathcal{H}^2$, it is always well-defined for elements on the image of $\mathcal{H}^2$ by ε, and (c) $\gamma = \delta\varepsilon$. The closing defined by $\varphi = \varepsilon\delta$ is only partially defined.

4.2 Erosion and dilation in $\mathcal{F}(\Omega, \mathcal{H}^2)$

If $(\mathcal{H}^2, \leq)$ is a complete lattice, the set of images $\mathcal{F}(\Omega, \mathcal{H}^2)$ is also a complete lattice defined as follows: for all $f, g \in \mathcal{F}(\Omega, \mathcal{H}^2)$, (i) $f \leq g \Leftrightarrow f(p) \leq g(p)$, $\forall p \in \Omega$; (ii) $(f \wedge g)(p) = f(p) \wedge g(p)$, $\forall p \in \Omega$; (iii) $(f \vee g)(p) = f(p) \vee g(p)$, $\forall p \in \Omega$, where $\wedge$ and $\vee$ are the infimum and supremum in $\mathcal{H}^2$. One can now define the following adjoint pair of flat erosion $\varepsilon_B(f)$

and flat dilation $\delta_B(f)$ of each pixel p of the image f [20, 13]:

$$\varepsilon_B(f)(p) = \bigwedge_{q \in B(p)} f(p+q), \tag{23}$$

$$\delta_B(f)(p) = \bigvee_{q \in B(p)} f(p-q), \tag{24}$$

where the set B is called the structuring element, which defines the set of points in Ω when it is centered at point p, denoted $B(p)$ [22]. These operators, which are translation invariant, can be seen as constant-weight (this the reason why they are called flat) inf/sup-convolutions, where the structuring element B works as a moving window.

The above erosion (resp. dilation) moves object edges within image in such a way that expands image structures with values in $\mathcal{H}^2$ close to the bottom element (resp. close to the top) of the lattice $\mathcal{F}(\Omega, \mathcal{H}^2)$ and shrinks object with values close to the top element (resp. close to the bottom).

4.3 Opening and closing in $\mathcal{F}(\Omega, \mathcal{H}^2)$

Given the adjoint image operators $(\varepsilon_B, \delta_B)$, the opening and closing by adjunction of image f, according to structuring element B, are defined as the product operators [20, 13]:

$$\gamma_B(f) = \delta_B\left(\varepsilon_B(f)\right), \tag{25}$$

$$\varphi_B(f) = \varepsilon_B\left(\delta_B(f)\right). \tag{26}$$

Openings and closings are referred to as morphological filters, which remove objects of image f that do not comply with a criterion related, on the one hand, to the invariance of the object support to the structuring element B and, on the other hand, to the values of the object on $\mathcal{H}^2$ which are far from (in the case of the opening) or near to (in the case of the closing) to the bottom element of $\mathcal{H}^2$ according to the given partial ordering $\leq$.

Once the pairs of dual operators $(\varepsilon_B, \delta_B)$ and (γ_B, φ_B) are defined, the other morphological filters and transformation can be naturally defined [22] for images in $\mathcal{F}(\Omega, \mathcal{H}^2)$. We limit here the the illustrative examples with the basic ones.

4.4 Application to morphological processing univariate Gaussian distribution valued images

Example 1. A first example of morphological processing for images on $\mathcal{F}(\Omega, \mathcal{H}^2)$ is given in Fig. 6-7. The starting point is a standard gray-level image $g \in \mathcal{F}(\Omega, \mathbb{R})$, which will map to the image $f(p) = f_x(p) + if_y(p)$ by the following transformations: (1) the image is normalized to have zero mean and unit variance; (2) the real and imaginary components of $f(p)$ are obtained by computing respectively the mean and standard deviation over a patch centered

a P of radius W pixels (in the example $W = 4$); i.e.,

$$g(p) \mapsto \hat{g}(p) = \frac{g(p) - \mathrm{M}ean(g)}{\sqrt{\mathrm{V}ar(g)}} \mapsto f(p) = \mathrm{M}ean_W(\hat{g})(p) + i\sqrt{\mathrm{V}ar_W(\hat{g})(p)}.$$

Fig. 6-7 gives a comparison of morphological erosions $\varepsilon_B(f)(p)$ and openings $\gamma_B(f)(p)$ on this image f using the five complete (inf-semi)lattice of $\mathcal{H}^2$ considered in the paper. The same structuring element B, a square of 5×5 pixels, has been used for all the examples. First of all, we remind that working on the product complete lattice $(\mathcal{H}^2, \leq_{\mathcal{H}^2})$ is equivalent to a marginal processing of real and imaginary components. As expected, the symmetric ordering-based inf-semilattice $(\mathcal{H}^2, \preceq_{\mathcal{H}^2})$ and polar ordering-based lattice $(\mathcal{H}^2, \leq_{\mathcal{H}^2}^{pol})$ produce rather similar results for openings. We observe that in both cases the opening produces a symmetric filtering effect between bright/dark intensity in the mean and standard deviation component. But it is important to remark that the processing effects depend on how image components are valued with respect to the origin $z_0 = (0, 1)$. This is the reason why it is proposed to always normalize by mean/variance the image.

The results of the openings produced by working on geodesic lattice $(\mathcal{H}^2, \preceq_{\mathcal{H}^2}^{geo})$ and asymmetric geodesic lattice $(\mathcal{H}^2, \bigwedge_{\mathcal{H}^2}^{\vec{\to}+}, \bigvee_{\mathcal{H}^2}^{\vec{\to}+})$ involves a processing which is mainly driven by the values of the standard deviation. Hence, the filtering effects are potentially more interesting for applications requiring to deal with pixel uncertainty, either in a symmetric processing of both bright/dark mean values with $(\mathcal{H}^2, \curlyvee_{\mathcal{H}^2}^{geo})$ or in a more classical morphological asymmetrization with $(\mathcal{H}^2, \bigwedge_{\mathcal{H}^2}^{\vec{\to}+}, \bigvee_{\mathcal{H}^2}^{\vec{\to}+})$.

Example 2. Fig. 8 illustrates an example of image enhancement from a very noisy image $g(p)$. The noise is related to an acquisition at the limit of exposure time/spatial resolution. We consider an image model $f(p) = f_x(p) + if_y(p)$, where $f_x(p) = g(x)$ and $f_y(p)$ is the standard deviation of intensities in a patch of radius equal to 4 pixels centered a p. Results obtained from a closing $\varphi_B(f)(p)$ using the polar ordering-based lattice, the geodesic lattice $(\mathcal{H}^2, \curlyvee_{\mathcal{H}^2}^{geo})$ and the asymmetric geodesic lattice $(\mathcal{H}^2, \bigwedge_{\mathcal{H}^2}^{\vec{\to}+}, \bigvee_{\mathcal{H}^2}^{\vec{\to}+})$ are compared, where the structuring element B is a square of 5×5 pixels. In order to be able to compare them with a non morphological operator, it is also given the result of filtering by computing the minimax center in a square of 5×5 pixels [3, 1].

Example 3. The example given in Fig. 9 corresponds to an image $f(p) = f_x(p) + if_y(p)$ obtained by multiple acquisition of a sequence of $100 frames$, where $f_x(p)$ represents the mean intensity at each pixel and $f_y(p)$ the standard deviation of intensity along the sequence. The goal of the example is to show how to extract image objects of large intensity and support size smaller than the structuring element (here a square of 7×7 pixels) using the residue between the original image $f(p)$ and its filtered image by opening $\gamma_B(f)$. In the case of images on $\mathcal{F}(\Omega, \mathcal{H}^2)$, the residue is defined as the pixelwise hyperbolic distance between them. In this case study, results on processing on polar ordering-based lattice versus asymmetric geodesic lattice are compared.

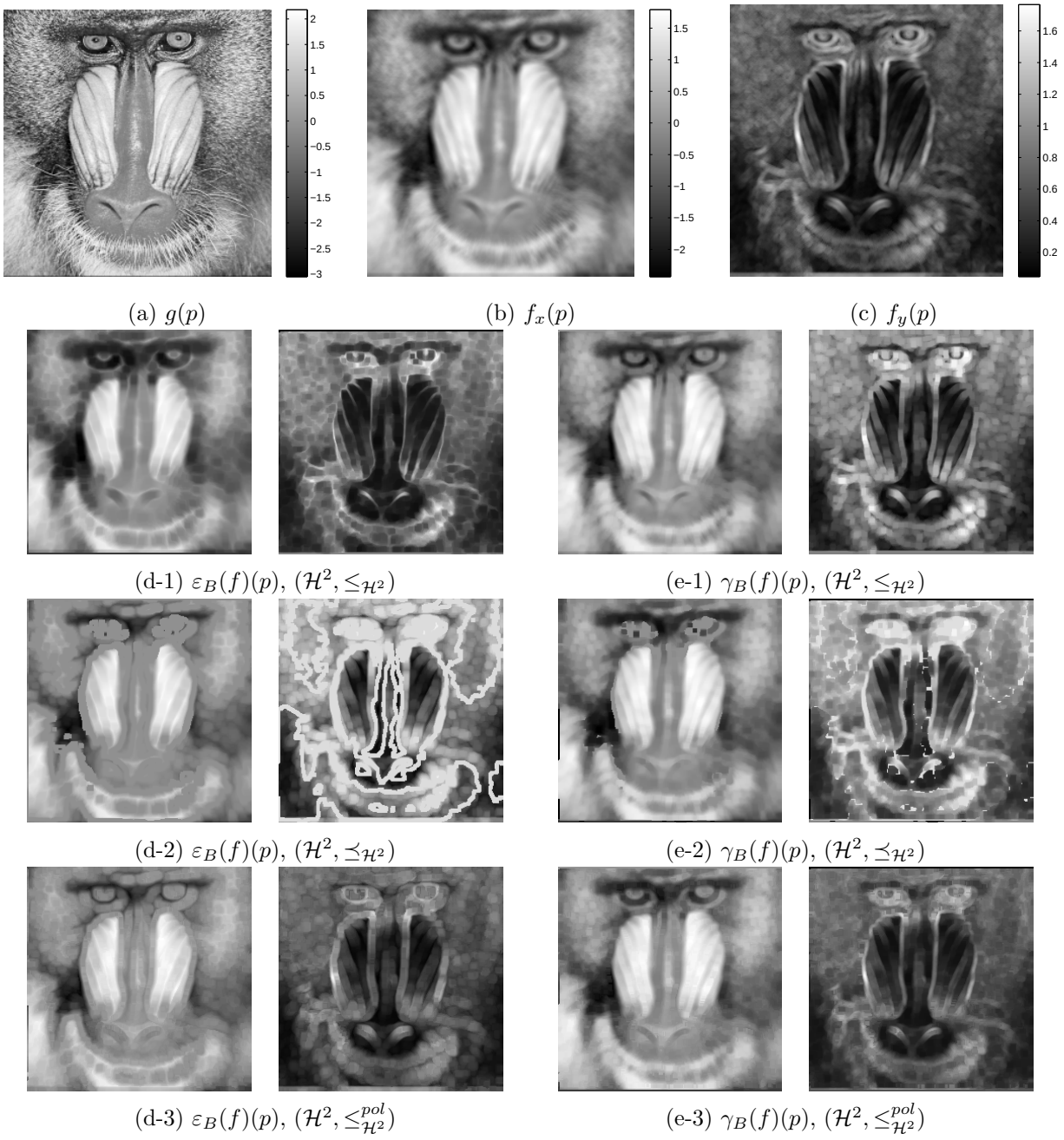

Figure 6: Comparative of morphological erosions and openings of an image $f \in \mathcal{F}(\Omega, \mathcal{H}^2)$: (a) Original real-valued image $g(p) \in \mathcal{F}(\Omega, \mathbb{R})$ used to simulate (see the text) the image $f(p) = f_x(p) + i f_y(p)$, where (b) and (c) gives respectively the real and imaginary components. (d-) and (e-) depict respectively the erosion $\varepsilon_B(f)(p)$ and opening $\gamma_B(f)(p)$ of image $f(p)$ for five orderings on the upper half-plane. The structuring element B is a window of 5×5 pixels. Continued in next figure.

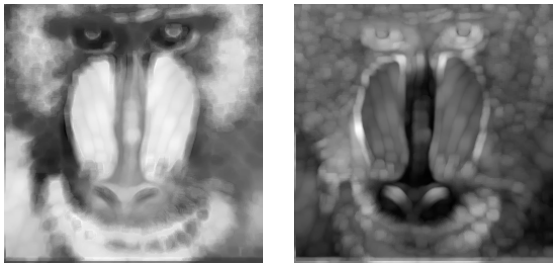

(d-4) $\varepsilon_B(f)(p)$, $(\mathcal{H}^2, \preceq^{geo}_{\mathcal{H}^2})$

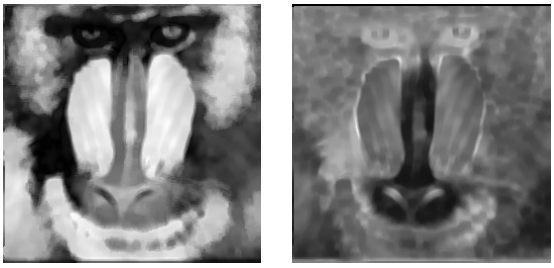

(e-4) $\gamma_B(f)(p)$, $(\mathcal{H}^2, \preceq^{geo}_{\mathcal{H}^2})$

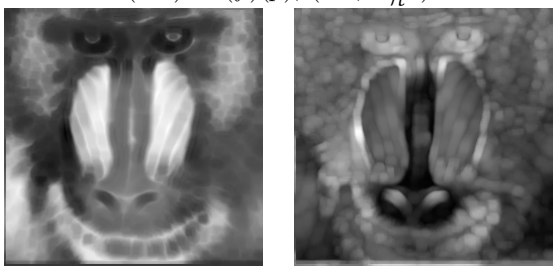

(d-5) $\varepsilon_B(f)(p)$, $(\mathcal{H}^2, \bigwedge^{\overrightarrow{-}\to+}_{\mathcal{H}^2}, \bigvee^{\overrightarrow{-}\to+}_{\mathcal{H}^2})$

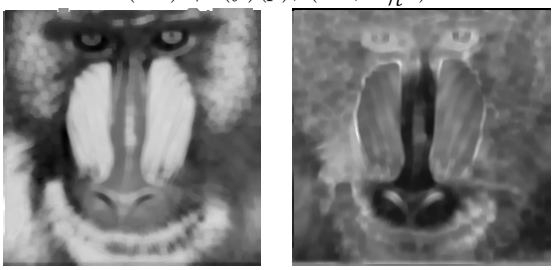

(e-5) $\gamma_B(f)(p)$, $(\mathcal{H}^2, \bigwedge^{\overrightarrow{-}\to+}_{\mathcal{H}^2}, \bigvee^{\overrightarrow{-}\to+}_{\mathcal{H}^2})$

Figure 7: Continuation from previous figure.

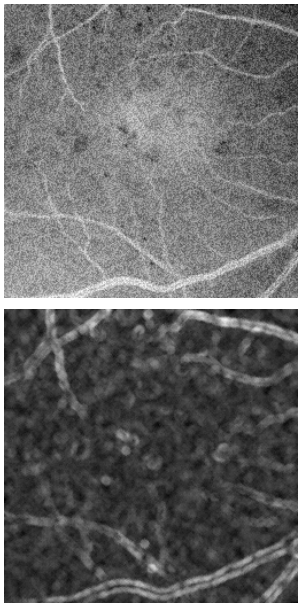

(a) $f(p)$

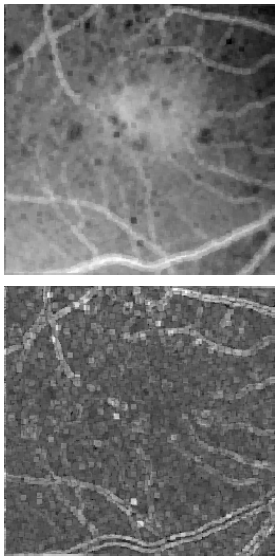

(b) Minimax center 5×5

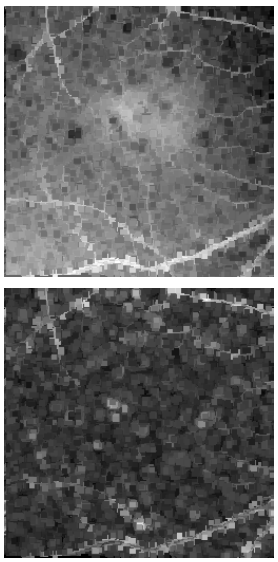

(c) $\varphi_B(f)(p)$, $(\mathcal{H}^2, \leq^{pol}_{\mathcal{H}^2})$

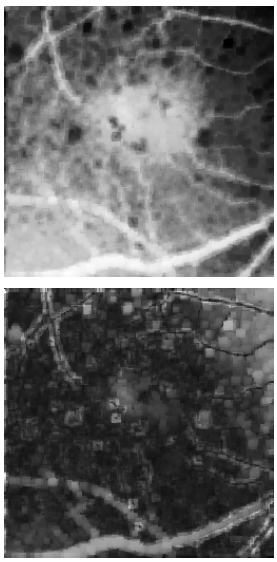

(d) $\varphi_B(f)(p)$, $(\mathcal{H}^2, \preceq^{geo}_{\mathcal{H}^2})$

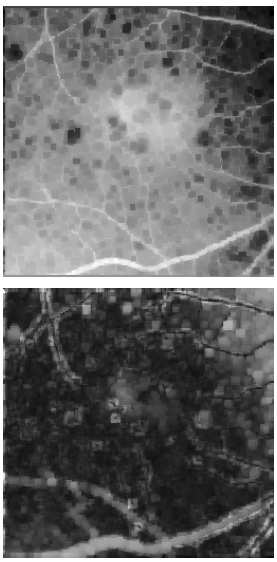

(e) $\varphi_B(f)(p)$, $(\mathcal{H}^2, \bigwedge^{-\to+}_{\mathcal{H}^2}, \bigvee^{-\to+}_{\mathcal{H}^2})$

Figure 8: Morphological processing of Gaussian distribution-valued noisy image: (a) Original image $f \in \mathcal{F}(\Omega, \mathcal{H}^2)$, showing both the real and the imaginary components; (b) filtered image by computing the minimax center in a square of 5×5 pixels; (c) morphological closing working on the polar ordering-based lattice; (d) morphological closing working on the geodesic lattice; (e) morphological closing on the asymmetric geodesic lattice. In both cases the structuring element B is also a square of 5×5 pixels.

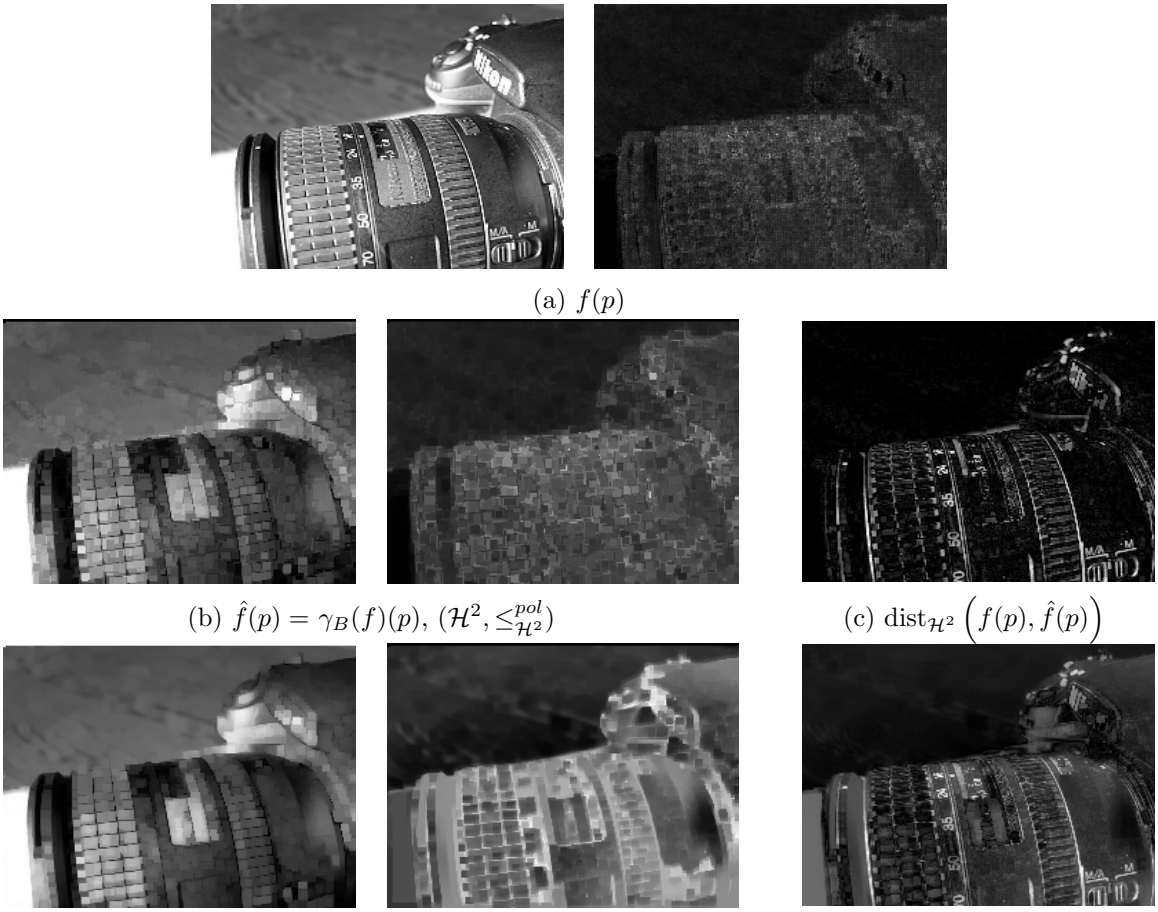

(a) $f(p)$

(b) $\hat{f}(p) = \gamma_B(f)(p)$, $(\mathcal{H}^2, \leq^{pol}_{\mathcal{H}^2})$

(c) $\mathrm{dist}_{\mathcal{H}^2}\left(f(p), \hat{f}(p)\right)$

(d) $\check{f}(p) = \gamma_B(f)(p)$, $(\mathcal{H}^2, \bigwedge^{-\to+}_{\mathcal{H}^2}, \bigvee^{-\to+}_{\mathcal{H}^2})$

(e) $\mathrm{dist}_{\mathcal{H}^2}\left(f(p), \check{f}(p)\right)$

Figure 9: Morphological detail extraction of multiple acquisition image modeled as a Gaussian distribution-valued: (a) Original image $f \in \mathcal{F}(\Omega, \mathcal{H}^2)$, showing both the real and the imaginary components; (b) morphological opening $\gamma_B(f)$ working on polar ordering-based lattice; (c) corresponding residue (pixelwise hyperbolic difference) between the original and the opened image; (d) morphological opening $\gamma_B(f)$ working on the asymmetric geodesic lattice; (e) corresponding residue. In both cases the structuring element B is also a square of 7×7 pixels.

5 Perspectives

Discussed partial orders and corresponding morphological operators can be applied to process other hyperbolic-valued images. For instance, on the one hand, it was proved in [6] that the structure tensor for 2D images, i.e., at each pixel is given a 2×2 symmetric positive definite matrix whose determinant is equal to 1, are isomorphic to the Poincaré unit disk model. On the other hand, polarimetric images [9] where at each pixel is given a partially polarized state can be embedded in the Poincaré unit disk model. In both cases, we only need the mapping from the Poincaré disk model to the Poincaré half-plane, i.e., $z \mapsto -i\frac{z+1}{z-1}$.

Levelings are a powerful family self-dual morphological operators which have been also formulated in vector spaces [16], using geometric notions as minimum enclosing balls and half-planes intersection. We intend to explore the formulation of levelings in the upper half-plane in a future publication.

References

[1] M. Arnaudon, F. Nielsen. On approximating the Riemannian 1-center. *Computational Geometry,* Vol. 46, No. 1, 93–104, 2013.

[2] S. Amari, H. Nagaoka. *Methods of Information Geometry, Translations of Mathematical Monographs.* Vol. 191, Am. Math. Soc., 2000.

[3] M. Bădoiu, K.L. Clarkson. Smaller core-sets for balls. In *Proc. of the fourteenth annual ACM-SIAM symposium on Discrete algorithms (SIAM)*, pp. 801–802, 2003.

[4] V. Cammarota, E. Orsingher. Travelling Randomly on the Poincaré Half-Plane with a Pythagorean Compass. *Journal of Statistical Physics,* Vol. 130, No. 3, 455–482, 2008.

[5] J.W. Cannon, W.J. Floyd, R. Kenyon, W.R. Parry. *Hyperbolic Geometry.* Flavors of Geometry, MSRI Publications, Vol. 31, 1997.

[6] P. Chossat, O. Faugeras. Hyperbolic Planforms in Relation to Visual Edges and Textures Perception. *PLoS Computational Biology,* Vol. 5, Issue 12, p1, 2009.

[7] S.I.R. Costa, S.A. Santos, J.E. Strapasson. Fisher information matrix and hyperbolic geometry. In *Proc. of IEEE ISOC ITW2005 on Coding and Complexity,* pp. 34–36, 2005.

[8] S.I.R. Costa, S.A. Santos, J.E. Strapasson. Fisher information distance: a geometrical reading, *arXiv:1210:2354v1,* 15 p., 2012.

[9] J. Frontera-Pons, J. Angulo. Morphological Operators for Images Valued on the Sphere. In *Proc. of IEEE ICIP'12 (2012 IEEE International Conference on Image Processing)*, pp. 113–116, Orlando (Florida), USA, October 2012.

[10] L. Fuchs. *Partially ordered algebraic systems.* Pergamon, 1963.

[11] A.K. Guts. Mappings of families of oricycles in Lobachevsky space. *Math. USSR-Sb.,* Vol. 19, 131–138, 1973.

[12] A.K. Guts. Mappings of an ordered Lobachevsky space. *Siberian Math. J.,* Vol. 27, No. 3, 347–361, 1986.

[13] H.J.A.M. Heijmans. *Morphological image operators.* Academic Press, Boston, 1994.

[14] H.J.A.M. Heijmans, R. Keshet. Inf-semilattice approach to self-dual morphology. *Journal of Mathematical Imaging and Vision,* Vol. 17, No. 1, 55–80, 2002.

[15] R. Keshet. Mathematical Morphology on Complete Semilattices and its Applications to Image Processing. *Fundamenta Informaticæ,* Vol. 41, 33–56, 2000.

[16] F. Meyer. Vectorial Levelings and Flattenings. In *Mathematical Morphology and its Applications to Image and Signal Processing (Proc. of ISMM'02),* Kluwer, pp. 51–60, 2000.

[17] F. Nielsen, R. Nock. On the smallest enclosing information disk. *Information Processing Letters,* Vol. 105, 93–97, 2008.

[18] F. Nielsen, R. Nock. Hyperbolic Voronoi diagrams made easy. In *Proc. of the 2010 IEEE International Conference on Computational Science and Its Applications,* pp. 74–80, 2010.

[19] L. Sbaiz, F. Yang, E. Charbon, S. Süsstrunk, M. Vetterli. The Gigavision Camera. In *Proc. of IEEE ICASSP'09,* pp. 1093–1096, 2009.

[20] J. Serra. *Image Analysis and Mathematical Morphology. Vol II: Theoretical Advances,* Academic Press, London, 1988.

[21] M. Shaked, J. G. Shanthikumar. *Stochastic Orders and their Applications,* Associated Press, 1994.

[22] P. Soille. *Morphological Image Analysis.* Springer-Verlag, Berlin, 1999.